The Sixteenth International Congress on Sound and Vibration
Kraków, 5-9 July 2009

NUMERICAL PREDICTION OF COMBUSTION INDUCED VIBRO-ACOUSTICAL INSTABILITIES IN A GAS TURBINE COMBUSTOR

Artur Pozarlik, Jim Kok

University of Twente, P.O.Box 217, 7500 AE Enschede, The Netherlands
e-mail: a.k.pozarlik@utwente.nl

Introduction of lean premixed combustion to gas turbine technology reduced the emission of harmful exhaust gas species, but due to the high sensitivity of lean flames to acoustic perturbations, the average life time of gas turbine engines was decreased significantly. Very dangerous to the integrity of the gas turbine structure is the mutual interaction between combustion, acoustics and wall vibration. This phenomenon can lead to a closed loop feedback system, with as a result fatigue failure of the combustor liner and fatal damage to the gas turbine rotor.
In this paper the use of numerical tools for CFD and CSD analysis is described to predict the hazardous frequencies at which the instabilities can occur. The two way interaction of the combustible compressible flow and structural walls is investigated with the application of the partitioning fluid-structure interaction approach. In this technique the fluid and structural model are considered as individual but coupled dynamic systems. Information of conditions at the fluid-structure interface is exchanged at given time steps through the interface connection created between the numerical domains. Therefore, the partitioned approach can take the full advantage of existing, well developed and tested codes for both, fluid and structure analysis. Next to the fluid-structure interaction analysis, acousto-elastic and modal models are applied to get insight into the acoustic and vibration pattern during the instability process. The calculations use elements devoted to the solution of the acoustic and structural fields. This approach has the advantage of high resolution of the acoustics, but takes into account only one way combustion dynamics (taken from the CFD results).
All numerical solutions are compared to experimental results obtained on a laboratory test rig. The data is evaluated for both, pressure and velocity fields.

1. Introduction

Each flame posses an intrinsic instability which leads to the noise generation. However, different sources of noise generation by flame can be distinguished: the autonomous noise is a product of the flame instabilities only; the coupled noise is an effect of the mutual interaction between flame and acoustic waves. The latter is of a great importance in a gas turbine industry as it can lead to the thermo-acoustics instabilities and, after coupling with walls vibration, to fatigue failure of the combustion system. The genesis of the thermo-acoustics instabilities growing up effect was first described by Lord Rayleigh[1]. His criterion with later changes[2] states that the instabilities are promoted when the heat fluctuations released by the flame and pressure changes are in phase and energy gain exceed energy losses to the wall, see Eq. 1.

$$\frac{(\gamma-1)}{\gamma p_0}\int_V \int_0^\tau p'Q'dtdV > \int_A \int_0^\tau p'\boldsymbol{u}dtdA \qquad \text{Eq. 1}$$

During the lean combustion, the turbulent flame with its enormous thermal power amplifies acoustic pressure changes inside the combustion chamber. The combustion chamber is acoustically closed and only small part of the sound is able to leave it together with an exhaust gases. Since dissipation of the pressure wave in the chamber is not significant, most of the sound is reflected from walls and impinging flame, which is highly sensitive on acoustic perturbations. The acoustic source, i.e. flame, is modified by the reflected waves and it produces even stronger pressure fluctuations inside the combustion chamber. In a case when self-excited instabilities arise in the system, especially when their frequency is nearby, or even matched with the resonant frequency of the combustion chamber walls, the amplitude of wall vibration is enhanced significantly. Furthermore, the high temperature of the environment, the liner operates in, has negative impact on the walls strength and performances. Those factors, i.e. high amplitude of vibrations and reduced material properties of the liner, combined with long operational time without any maintenance or overhaul lead finally to the fatigue damage of the liner[3].

Next to liner fatigue damage, the thermo-acoustic instabilities are also a source of many other undesirable effects occurring in the combustion chamber during the combustion process, like enhanced heat transfer to the walls, flashback or blow off. Therefore, investigation and prediction possible thermo-acoustic instabilities are of a great importance in gas turbines technologies.

2. Experiment

The combustion setup investigated here is a laboratory scale part of the real gas turbine combustion chamber. Because of the significant geometrical dimensions and high operational costs, it was unpractical to build the whole combustion chamber together with 24 burners. Instead, the chamber with only one burner and thermal power reduced to 500 kW at 5 bar absolute pressure was manufactured. In order to match acoustical and structural eigenfrequencies with the one occur in the full scale device, the geometrical dimensions of the investigated setup were modified. The investigated flame is a natural gas lean premixed flame. Stabilization of flame is done by inner and outer recirculation regions created by swirl tube. Between the liner and pressure vessel, the cooling flow is present to decrease the overall liner temperature. Several pressure transducers and thermocouples are located along the combustion test rig to monitor pressure and temperature changes during different operating conditions. For the pressure measurements, Kulite pressure sensors with measurement range of 0-0.35 bar are used. To decrease the risk of sensor damage due to high temperature, the pressure transducers are mounted on the side tubes and cooled by external air flow. The side tubes are connected to the semi-infinity hoses. At the end of each hose material absorbing acoustic wave is used. Therefore, the sensors can read the pressure changes which are in the combustion chamber without errors made by resonance inside the tube or hose. To observe flame and measure its properties, the setup is equipped with a system of windows. Chemiluminescence and Planer Laser Induced Fluorescence (PLIF) are used to gather information about flame. The measurements of the liner vibrations are done on the part of the liner with higher flexibility. This section has decreased thickness. This makes any variations in the pressure amplitude or frequency inside the combustion chamber, directly translated to change of the liner vibration pattern. Furthermore, the flexible section located between stiff liner plates gives well defined boundary conditions for the numerical models. All thermocouples and pressure transducers are placed in certain distance from the flexible liner to preserve free vibration pattern. The Laser Doppler Vibrometer allows high accuracy measurements of the hot liner surface without contact with it. Measurements are performed along slit window, because due to high length/width ratio of the liner, only longitudinal modes are expected. Data from the pressure, velocity and temperature sensors are collected by Labview and Siglab data acquisition systems. Location of each sensor is presented on Fig. 1.

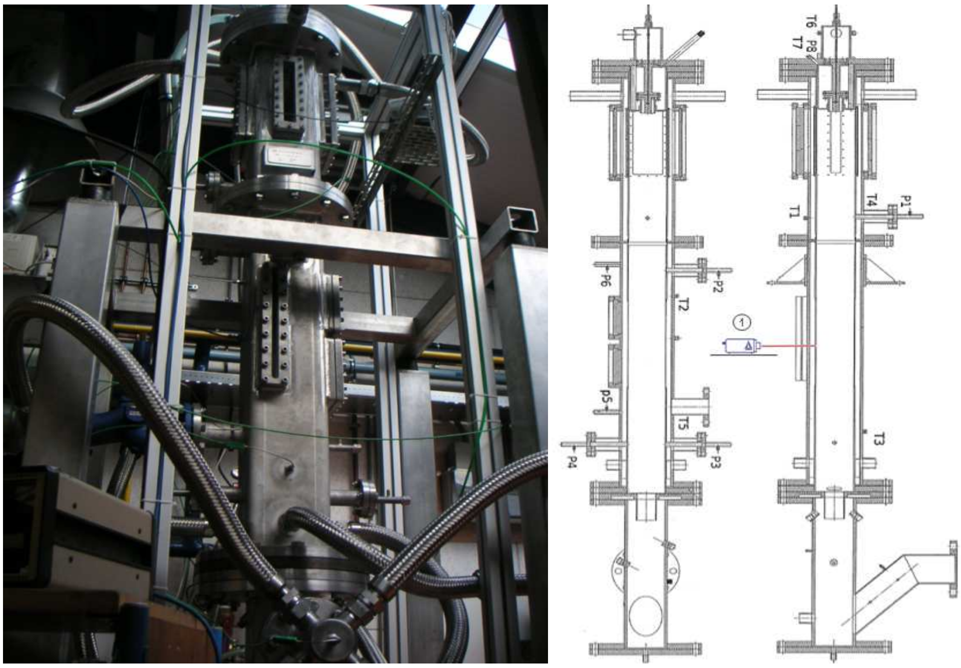

Fig. 1. Combustion setup (left), drawing of the setup with data collection points (right), where: T1-T7 are thermocouples, P1-P6 are pressure transducers and 1 is the Laser Doppler Vibrometer.

For measurements with pulsating equivalence ratio a MOOG valve is used. The MOOG valve perturbs the mass flow of fuel in a controlled way. Experiment operating conditions and liner dimensions are depicted in Tab. 1.

Combustion flow						
Power	Abs. pressure	Air factor	Mass flow rate	Air temp.	Pulsation freq.	Pulsation amp.
125 kW	1.5 bar	1.8	75.53 g/s	573 K	300 Hz	8.5 %
Dimensions and material properties of the liner						
Length total/flexible part	Thickness stiff part/flexible part	Width	Density	Young's modulus	Poisson's ratio	
1.813 / 0.400 m	0.004 / 0.0015 m	0.150 m	7844 kg/m^3	138 GPa	0.3	

Tab. 1. Operational parameters during combustion process and liner dimensions

3. Numerical approach

Three different numerical approaches are employed to predict the hazardous instabilities and liner vibrations in the combustion system. All models are based on coupled and uncoupled CFD and CSD simulations.

3.1 Fluid-Structure Interaction

The partitioned approach is used here to solve the fluid-structure interaction problem. In this approach fluid and structural model are considered as an isolated entities. This allows using independent techniques to solve fluid and structure subdomains along the fluid-structure interface at a given time[4]. Thus, the partitioned approach can take the full advantage of existing, well developed and tested codes for both, fluid and structure analysis. The disadvantage of this approach is the necessity of using additional code, which provides coupling interface between investigated models. The data send through the interface can be contaminated by the errors created during mapping and interpolating procedures. The partitioning approach can be solved in serial or parallel way and the fields can be coupled weakly or strongly. The serial weak coupling, where fluid and structural solver works alternately, is used here. Both fields are solved in successive steps and the coupling is done at the end of the time step. During the call, solutions of one process are used as boundary conditions for the other process. The serial weak coupling is very efficient technique as calculation time and computer power demands are much smaller than during strong coupling, where data is exchanged every sub-iteration. The weak coupling method is devoted for the coupled fields with significant difference in density or characteristic timescale, as well, when the displacement of the structure is minor[5]. All three conditions are fulfilled in case of interaction analysis in combustion chamber. The parallel weak coupling has advantage in a shorter calculation time, in comparison to serial coupling. However, it can destabilize the solution process as less recent results are applied in each field solver[6].

To exam coupling between combustion, acoustics and vibrations, three different numerical codes are combined into one calculation process. For the turbulent flow, heat transfer and combustion of the reacting mixture calculations Ansys CFX 11 is used. Acoustic wave created by an oscillating flame is solved during the CFD computations, as well. The structural vibrations analysis is performed using Ansys Multiphysics 11 commercial code. The interface connection between both codes is ensured by the MFX coupling interface code. Data exchange is done in two-way manner. The two-way interaction method allows pressure and displacement information exchange between CFD and CSD numerical solver. The physical process investigated here is driven by combustion instabilities, thus combustible fluid flow process is resolved first. Graphical interpretation of partitioned coupling and serial F→S coupling is presented on Fig. 2.

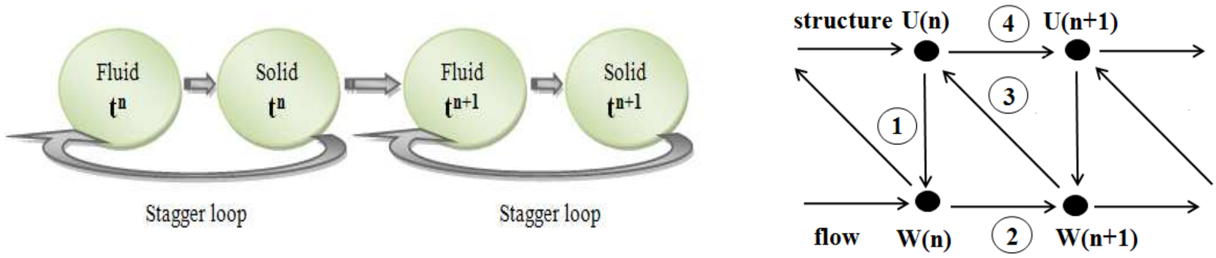

Fig. 2. Partitioned coupling approach (left) and serial S→F coupling

The dynamic system behaviour including interaction between domains can be written in a matrix form according to Eq. 2.

$$\begin{bmatrix} \boldsymbol{M_s} & \boldsymbol{0} \\ \boldsymbol{\rho_f R^T} & \boldsymbol{M_f} \end{bmatrix} \begin{bmatrix} \ddot{\boldsymbol{u}} \\ \ddot{\boldsymbol{p}} \end{bmatrix} + \begin{bmatrix} \boldsymbol{C_s} & \boldsymbol{0} \\ \boldsymbol{0} & \boldsymbol{C_f} \end{bmatrix} \begin{bmatrix} \dot{\boldsymbol{u}} \\ \dot{\boldsymbol{p}} \end{bmatrix} + \begin{bmatrix} \boldsymbol{K_s} & \boldsymbol{-R} \\ \boldsymbol{0} & \boldsymbol{K_f} \end{bmatrix} \begin{bmatrix} \boldsymbol{u} \\ \boldsymbol{p} \end{bmatrix} = \begin{bmatrix} \boldsymbol{f_s(t)} \\ \boldsymbol{f_f(t)} \end{bmatrix} \qquad \text{Eq. 2}$$

Where: Matrix ***M*** stands for mass matrix, ***C*** for damping matrix, ***K*** for stiffness matrix and ***R*** is coupling matrix. Nodal displacement vector is marked as ***x*** and time dependent load vector by ***f(t)***. Subscripts *f* and *s* stand for fluid and structure, respectively.

The mesh on the both side of the interface connection is usually not conforming. In most of cases, the elements density and the elements shape of fluid and structural mesh are not coincidence spatially. In case the liner mesh is finer on the sender side a globally conservative interpolation method is used. In opposite case, a profile preserving interpolation method is applied. A bucket search algorithm is used for mesh mapping. All algorithms are standard available in the FEM Ansys package[6].

For the CFD computation, the Scale Adaptive Simulation also known as SAS is used. This model was introduced first by Menter et al[7]. The SAS formulation provides a turbulent length-scale, which is not proportional to the thickness of the turbulent layer, but it is proportional to the local flow structure. Standard turbulence models, on the other hand, always provide a lengths-scale proportional to the thickness of the shear layer. They do not adjust to the local flow topology and are therefore overly diffusive[7]. For the reacting flow calculations, standard CFX single-step Eddy Dissipation/Finite Rate Chemistry (ED/FRC) model of a reaction is used[8]. In ED/FRC model, the reaction rate is limited by turbulence quantities or by mixing, depending on the local Damköhler number. Thus while the rate for one step may be limited by the chemical kinetics, some other step might be limited by turbulent mixing.

To save computation time and to increase the number density of elements, the computational domain was reduced to a quarter section of the real combustion chamber, with periodic boundary conditions. A total number of 720 000 unstructured elements, mostly placed in the flame and recirculation region are used for calculations. The near-wall region is created with the use of prism elements to avoid generation of highly distorted tetrahedral elements at the face. The velocity and turbulence profiles at the inlet are taken from the steady-state calculations of the full setup geometry. The static average pressure is imposed at the combustion chamber outlet. Heat transfer coefficient is imposed on the investigated wall. Other walls have adiabatic and no-slip conditions. The influence of the pressure from the cooling passage is neglected. The total calculation time was equal to 80 ms with time step 1e-4s.

The structural model is simplified to one wall with flexible section. The calculations are performed with uniform material properties adequate to work at 760 ^{o}C. Mechanical loads from the CFX calculation are transferred to the internal liner face. A total number of 19 000 uniformly distributed SOLID92 tetrahedral elements is used for the dynamic calculation. Time step and total calculation time are the same as in the CFD calculation.

3.2 Acousto-elastic interaction and modal analysis

The acousto-elastic analysis is devoted to investigate mutual interaction between moving walls and acoustic field. The interaction between structure and acoustic field is especially significant when acoustic fluid is enclosed by the flexible structure. In case of acoustic fluid trapped in combustion chamber domain only the compressibility and inertia effect plays a major role. The presence of the hot air trapped by surrounding structure changes the physical behaviour of the system. The air introduces additional mass, stiffness and damping[9]. The acousto-elastic model includes gases with a mean temperature adequate to the gas temperature during the combustion cycle and liner material properties similar to one during the operating conditions. To simulate acoustic wave in the combustion chamber acoustic elements FLUID30 are employed. For the structure, SHELL63 elements with the element real constant equal to the material thickness are used. Between those two types, elements design to recognize structure on one side and fluid on other are placed. This configuration assures correct data transfer between the acoustic and structural elements. The geometry is simplified to the rectangular shape without the exhaust pipe. The reflection coefficient is calculated based on change in the cross-section area and imposed as end acoustic conditions. At the inlet, an acoustically hard wall is imposed. The pressure fluctuations are taken from the CFD analysis. The typical acoustic field created by acoustic source can be divided into two main regions: the near field and the far field acoustics. The near field acoustics is located in the vicinity of the acoustic source and strongly depends on the source properties. The far field zone starts at a certain distance from the source. Beyond the point of transition between the near field and far filed acoustics, the wave distribution is mainly independent on the distance from the source. Several definitions of the transition point between near and far field acoustics exists depends on the relation between dimensions of the source and the wave length, diffraction or the type of the acoustic source[10]. The direct prediction of the far field acoustics by the CFD computation is difficult to achieve, mainly due to requirements of meshing and time step. The CFD mesh must span all the way to the reception points with enough spatial resolution to directly resolve acoustic waves over the propagation distance with minimal to no numerical damping. However, the CFD results shown that in the investigated combustion chamber, in some distance behind the monopole source (i.e. flame), the pressure fluctuations are one-dimensional, see Fig. 3. Therefore the CFD domain is truncated in the vicinity of the flame, and pressure fluctuations are exported to acousto-elastic model, as shown on Fig. 3. The truncation distance is chosen close to flame, to preserve pressure signal no contaminated by the numerical errors.

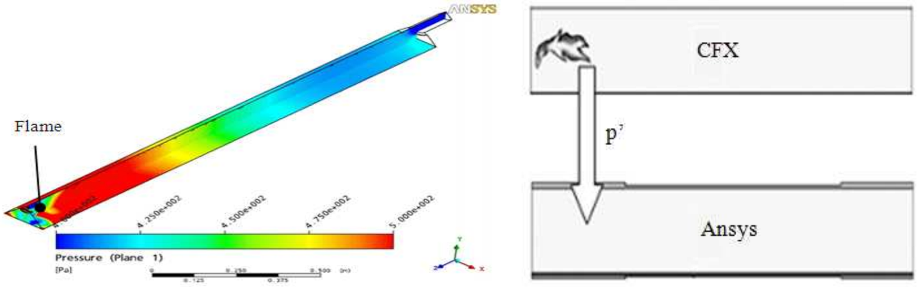

Fig. 3. One dimensional pressure change pattern (left), and acousto-elastic interaction (right)

Next to acousto-elastic interaction a modal analysis is performed. The vibration characteristics of the combustion chamber and the influence of the hot gases trapped inside are investigated. The eigenfrequencies and shape of the coupled modes are compared with each other and a relation between them is observed. The numerical model is the same as for the acousto-elastic investigation, except the pressure field exported from the CFX code and a reflection factor, which are not applied here.

4. Results

The results of the experiment are evaluated for pressure at location of pressure transducers P2 and for the liner velocity in the middle of the liner flexible section. Signal for experimental frequency spectra was averaged over 40 measurements, whereas for the time signal, only the most recent result was recorded. The experimental results are compared to the numerical data. Moreover, the modal analysis presents the shape of the coupled modes of the whole system.

During the fluid-structure interaction computation, the partitioning error can occur. To exam the influence of the error, the mesh displacement on the CFX side is compared to original displacement calculated by the structural code. As can be seen on Fig. 4, the coupling algorithm works well. Displacements on the structural and fluid face are the same and only minor errors are visible.

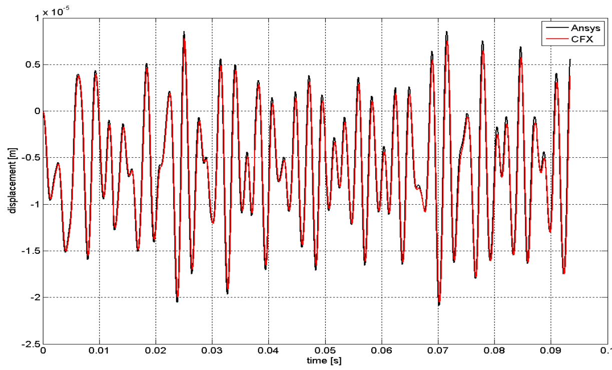

Fig. 4. Data transfer through the interface connection

The experimental and numerical results of the pressure changes show good agreement. The numerical amplitude of the pressure fluctuations has the same order as the experimental one. The numerical results are under-predicted only by factor 1.5-2, depends on the investigated model, see Fig. 5. This behaviour is caused by the numerical dispersion and dissipation of the acoustic wave during the CFD computations. Also, it is possible that because of very short calculation time (80 ms) the instabilities has no time to grow up to the limit observed during the experiment. Introduction of finer mesh and longer calculation time should improve results, but would also enormously increase the total calculation time. The thermo-acoustic instabilities observed during the experiment are located at 439 Hz and 640 Hz. Both numerical models predicted those peaks at 437 Hz and 625 Hz, which means that the acoustics, combustion and mean temperature field during numerical calculation is resolved correctly. However, due to the reasons described above, the power of the instabilities is under-predicted. The main peak visible during the numerical computations is located at 300 Hz and it comes from the frequency of fuel-to-air equivalence ratio pulsations.

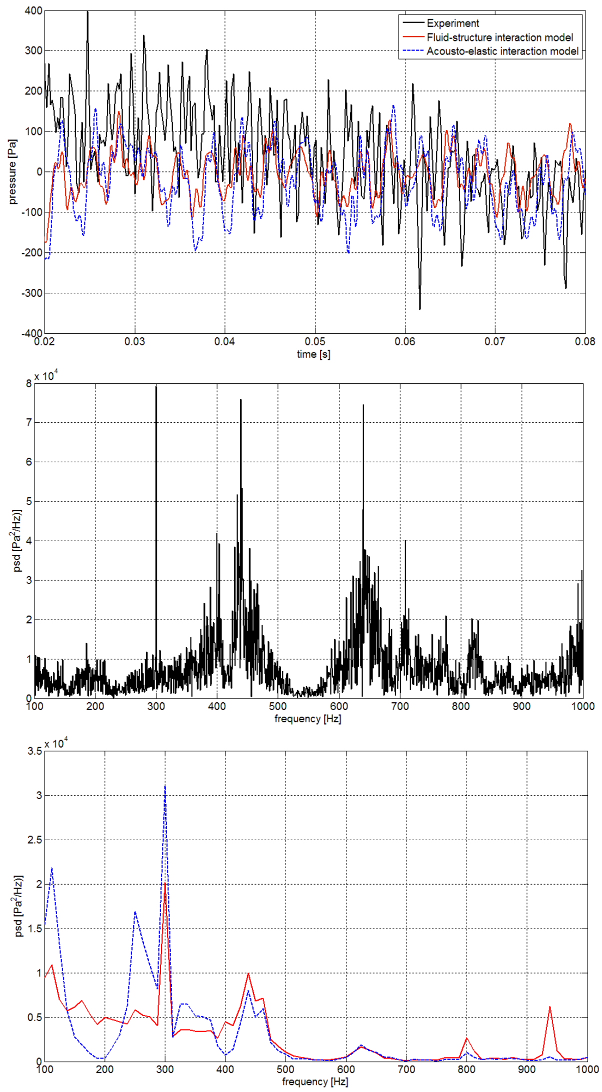

Fig. 5. Pressure changes: experimental and numerical results in time domain (top), experimental results in frequency domain (middle), numerical results in frequency domain (bottom).

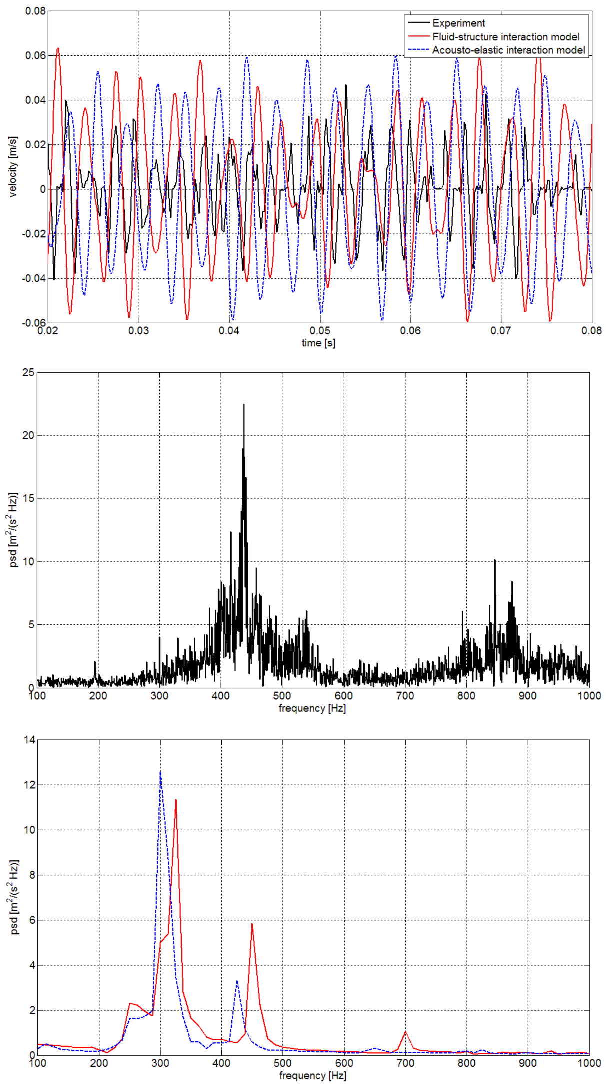

Fig. 6. Velocity changes: experimental and numerical results in time domain (top), experimental results in frequency domain (middle), numerical results in frequency domain (bottom).

The same behaviour as in case of pressure fluctuations is observed for the liner vibrations. The maximum numerical amplitude of the vibrations, is similar to the one recorded by Laser Doppler Vibrometer. The over-prediction visible on Fig. 6, is most likely a consequence of not including any damping to the material properties of the liner. Also cooling passage with cold air on the other side of the liner is not investigated here. But it could give additional damping factor. The frequency spectrum of the acousto-elastic model shows the hazardous instability at 435 Hz, whereas instabilities predicted by fluid-structure interaction model are located at 325 Hz and 450 Hz. Both spectra predicted peaks close to the experimental spectrum, which localized instabilities at 438 Hz and 846 Hz. In all investigated cases the forcing peak at 300 Hz is also visible.
Next to fluid-structure interaction and acousto-elastic analysis, the modal analysis is performed. The coupled modes are investigated in the range up to 700 Hz. Eight of them shows strong coupling between acoustic and structural domain, see Fig. 7. However, only half of them represent a pattern in which entrapped hot air is highly compressed or rarefied. Those modes are responsible for sig-

nificant volume changes in the system and as a consequence they can lead to the thermo-acoustic instabilities. All the eigenfrequencies of the volumetric modes match well with the frequency of the instability peaks observed during the experiment.

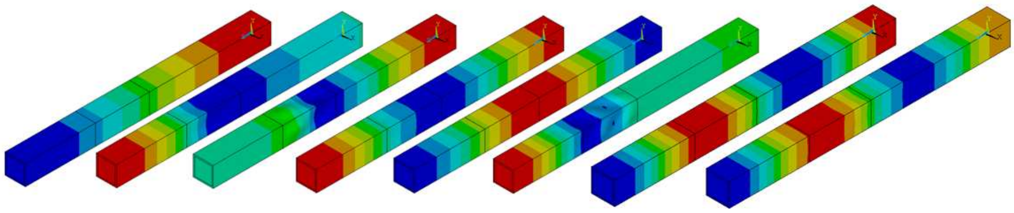

Frequency:	219 Hz	312 Hz	355 Hz	429 Hz	446 Hz	542 Hz	657 Hz	669 Hz

Fig.7. Coupled modes of the combustion chamber

5. Conclusions

Experimental and numerical investigation was done to investigate thermo-acoustic instabilities in the gas turbine combustion chamber. Three various numerical models with direct coupling between fluid and structural fields were used to predict the frequencies at which the instabilities can occur. The fluid-structure interaction, acousto-elastic and modal analysis show instabilities at 437 Hz, 437 Hz and 446 Hz, respectively. All those values are close to the thermo-acoustic instability observed during the experiment at 439 Hz. The frequency of liner vibration was predicted correctly as well. In case of pressure and velocity amplitude estimation, the numerical results differ from the experimental one, but the order of magnitude was preserved. The discrepancy between numerical results and experimental one comes mainly from numerical dispersion and dissipation, lack of physical damping in the investigated liner, lack of cooling passage model and short calculation time. Improving those factors should result in a better prediction not only of the frequency at which the instability occurs but also its amplitude.

Acknowledgment

This work is performed in the EU sponsored project FLUISTCOM in the Marie Curie Program, contract number MRTN-CT-2003-504183. The authors would like to thank CFX-ANSYS for the use of the code.

REFERENCES

1. J. Rayleigh, The Explanation of Certain Acoustic Phenomena, *Nature*,1878, 18, 319-321.
2. T. Poinsot, D. Veynante, *Theoretical and Numerical Combustion.* 2005, R.T. Edwards, Inc.
3. T. Tinga, J. van Kampen, B. de Jager, J. Kok, Gas Turbine Combustor Liner Life Assessment Using a Combined Fluid/Structural Approach. *Journal of Engineering for Gas Turbines and Power* , 2007, 129, 69-79.
4. C.A. Felippa, K.C. Park, C. Farhat, Partitioned analysis of coupled mechanical systems, *Computer Methods in Applied Mechanics and Engineering* , 2001, 190, 3247-3270.
5. B. Hubner, U. Seidel, Partitioned solution to strongly coupled hydroelastic systems arising in hydro turbine design, *2th IAHR Internaitonal Meeting of the Workgoup on Cavitation and Dynamic Problems in Hydraulic Machinery and Systems*, 2007, 55-64, Timisoara.
6. Ansys, *HTML Online Documentation*, Ansys Inc, 2007.
7. F.R. Menter, M. Kuntz, R. Bender, A scale-adaptive simulation model for turbulent flow prediction. *AIAA*, 2003.
8. CFX Ansys 11, *HTML Online Documentation*, Ansys Inc, 2007.
9. T.G. Basten, *Noise reduction by viscothermal acousto-elastic interaction in double wall panels*. 2001, PhD thesis, Enschede.
10. A.P. Dowling, J.E. Ffowcs Williams, *Sound and sources of sound.* 1983, Chichester: Ellis Horwood Publishers.